Penerbit Akademia Baru

Journal of Advanced Research in Fluid Mechanics and Thermal Sciences

Journal homepage: www.akademiabaru.com/arfmts.html
ISSN: 2289-7879

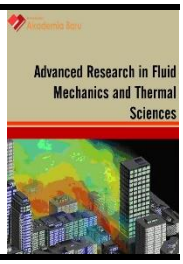

Effect of Biot Number on Convective Heat Transfer of Darcy-Forchheimer Nanofluid Flow over Stretched Zero Mass Flux Surface in the Presence of Magnetic Field

Open Access

Mohammed M. Fayyadh[1,*], Rozaini Roslan [1], R. Kandasamy [2], Inas R. Ali [1], Nisreen A. Hussein[3]

[1] Research Center of Computational Fluid Dynamics, Faculty of Applied Sciences and Technology, University Tun Hussein Onn Malaysia, Pagoh 84600, Johor, Malaysia
[2] Knowledge Institute of Technology India, Kalapalayan 637505, Tamilnadu, India
[3] Iraqi Ministry of Education, Babylon, Iraq

ARTICLE INFO

Article history:
Received 29 April 2019
Received in revised form 20 May 2019
Accepted 26 May 2019
Available online 15 July 2019

ABSTRACT

This work examined magneto-hydrodynamics flow of aluminum oxide– water based saturated in porous media that characterized by the Darcy-Forchheimer model. Heat transfer mechanism was analyzed in the presence of convective heating process and zero mass flux condition. Tiwari-Das model is employed to study the characteristics of nanofluid. A uniform magnetic field was imposed and a linear stretching surface was used to generate the flow. Application of appropriate transformation yields nonlinear ordinary differential equation through nonlinear Navier-Stokes equations and solved by Runge–Kutta Fehlberg shooting technique. Importance of influential variables such as velocity, temperature and concentration were elaborated graphically. Biot number, porosity, Forchheimer number and nanoparticle volume fraction parameters under various magnetic field and local Nusselt number were calculated numerically and interpreted. The results indicate that the effect of magnetic field is dominant on boundary layer thickness with respect to Biot number, porosity and nanoparticle volume fraction effect on temperature and nanoparticle concentration profile. An increase in Biot number, improvement in temperature distribution and nanoparticle concentration. The velocity distribution is decreased when there is an increase in the Forchheimer number and porosity parameters.

Keywords:
Heat transfer rate; Darcy – Forchheimer nanofluid flow; similarity transformation; magnetic field; Biot number

1. Introduction

The application of nanotechnology allows producing materials that have size less than 100 nm. These nanomaterials based on their structure and characteristics can be segmented into four categories: metal-based nanomaterials, carbon-based nanomaterials, composite and dendrimers. Choi *et al.,* [1] first evaluated the terminology nanofluid. Fluids that occupy particle sizes less than 100 nm can be termed as nanofluid. The categories of different nanoparticles are defined by particle

* *Corresponding author.*
E-mail address: abuzeen@gmail.com (Mohammed M. Fayyadh)

material, size, base fluid and concentration pertaining to the nanofluid. These nanoparticles could be suspended into any conventional fluid such as water, oil, ethylene glycol to form nanofluids. Nanoparticles offer better improvement in terms of thermo-physical characteristics over micro particles. The application of nanofluids ranges from enhancing efficiency of diesel generator to air conditioning cooling, power plant cooling, automotive, etc. Normally as heat transfer base fluids, water and ethylene glycol are employed. Nanoparticles are produced by employing various substances, which are generally segmented into metal-oxide (i.e. CuO, Al_2O_3), metallic (i.e. copper, aluminium) and different particles (i.e. carbon nanotubes) [2].

The investigators worldwide have gained a lot of interest in predicting the heat transfer behaviour because of its wide-scale engineering and biomedical applications such as heat conduction in tissues, heat pumps, energy creation, drug targeting, among others [3]. The well-known relation of heat conduction as advocated by Fourier is commonly used for defining heat transport characteristics. Later, Cattaneo generalised this relation through relaxation time. This factor was seen to overpower even the 'paradox of heat conduction'. Christov further generalised the idea of Cattaneo by replacing the time derivative with two Oldroyd upper-convected derivatives. Characterisation of this concept is done as Cattaneo–Christov or non-Fourier heat flux [4].

Investigation of flows saturating porous space has caught the attention of the researchers because of their key role in practical utilisations in industries and the field of engineering. In the available literature, much focus has been put on reporting the issues pertaining to permeable media that had been established by employing Darcy's relation, [5]. Forchheimer [6] employed the square velocity factor for Darcy's velocity expression in a bid to examine the boundary and inertia characteristics. Muskat [7] referred this term as Forchheimer that would always account for problems pertaining to high Reynolds number. Physically, quadratic drag for permeable space pertaining to the velocity expression can be delivered via higher filtration flow rates.

Non-Newtonian fluids are those that do not satisfy the classical Newton's law of viscosity in most of the industrial and technological applications. A single constitutive expression is not enough to describe the distinct features of all non-Newtonian fluids. Hence, to characterise the characteristics of non-Newtonian materials, the literature includes different models that have been designed. Some flow issues pertaining to Maxwell fluid were also evaluated by considering higher dimensions [8].

A mathematical model is presented for Darcy–Forchheimer by considering boundary layer flow pertaining to viscoelastic fluids over a linear stretching surface. We have considered flow models pertaining to elastic-viscous as well as second grade fluids [9].The Darcy–Forchheimer flow pertaining to viscous fluid was also examined over a curved stretching surface. The Darcy–Forchheimer relation is employed to define the flow in porous medium as well as the concept of heterogeneous and homogeneous reactions [10].

The water-based carbon nanotubes' steady two-dimensional (2D) flow can be attributed to a linear stretchable curved surface that is coiled around in the form of a circle with radius R. Hayat *et al.,* [11] took into account Darcy–Forchheimer porous medium as well as convective boundary condition. The Darcy–Forchheimer porous medium was employed for the two-dimensional flow of MWCNTs and SWCNTs [12]. The Darcy–Forchheimer 3D flow pertaining to water-based carbon nanomaterial (CNTs) was represented in a porous space via Darcy–Forchheimer expression. Convective heating was accounted to study the heat transfer mechanism. Alzahrani and Abdullah [13] performed a comparison of the results from single-wall (SWCNTs) and multi-wall carbon nanotubes (MWCNTs).

Evaluation of Darcy–Forchheimer flow pertaining to viscoelastic fluids was done subjected to Cattaneo–Christov heat flux as well as heterogeneous–homogeneous reactions. The Darcy–

Forchheimer model was accounted to characterise the flow in porous media. Hayat *et al.,* [14] used a modified version of Fourier's law via Cattaneo-Christov heat flux.

The current examination accounts for Darcy–Forchheimer flow pertaining to viscous fluid as a result of curved stretching sheet. Hayat *et al.,* [15] applied the heat transfer along with the Cattaneo–Christov theory to characterise the thermal relaxation characteristics. A description regarding the Cattaneo–Christov heat flux theory's role in two-dimensional laminar flow pertaining to the Jeffrey liquid has been provided with a vertical sheet. Meraj *et al.,* [16] employed a liquid with different thermal conductivity pertaining to the Darcy–Forchheimer porous space.

The distinct nanofluid models were put forward to describe the rheological characteristics and structure pertaining to such nanofluid. Researchers have gained a lot of interest in the rate and differential type models. The Maxwell model still widely employs the straightforward rate type nanofluid models. This model showed stress relaxation pertaining to various polymeric nanofluids. Few studies were referred in which the Maxwell model was employed under distinct flow configuration.

This research study is aimed at analysing the characteristics pertaining to magneto-hydrodynamics (MHD) and the Darcy–Forchheimer model that consider the flow of Maxwell nanofluid. We have considered Brownian motion, magnetic field, porosity with Nusselt number and thermophoresis with the impact of Biot number to address the heat transport mechanism. The mathematical development employed the boundary layer method. Strong nonlinear ordinary differential system can be established with appropriate variables. The numerical approach shooting technique along with Runge–Kutta–Fehlberg approach was employed in the development of convergent series solutions pertaining to temperature, velocity and concentration fields. The role of different pertinent parameters was investigated and described. The numerical data was considered for analysis, and computation of local Nusselt number was performed subsequently.

2. Modelling

In this paper, the steady two-dimensional (2D) stretched flow pertaining to Tiwari-Das nanofluid has been evaluated. The porous space is saturated via an incompressible nanofluid, which characterises the Darcy–Forchheimer model. A linear stretched sheet is responsible for the generation of flow. Imposing of a uniform magnetic field with strength B_o occurs towards the y-direction. The omission of induced magnetic field is characterised by a small magnetic Reynolds number. The implementation of the Cartesian coordinate is done in a manner in which x-axis is defined along the stretching sheet while the y-axis appears orthogonal to it. At y = 0, the stretching of the sheet is done along the x-direction given a velocity of u_w. A convective heating process is followed to manage the surface temperature as defined by heat transfer coefficient represented by h_f, while T_f signified the hot nanofluid's temperature under the sheet. The governing boundary layer can be represented as [17].

$$\frac{\partial u}{\partial x}+\frac{\partial v}{\partial y}=0 \tag{1}$$

$$u\frac{\partial u}{\partial x}+v\frac{\partial u}{\partial y}+\lambda_1\left(u^2\frac{\partial^2 u}{\partial x^2}+v^2\frac{\partial^2 u}{\partial y^2}+2uv\frac{\partial^2 u}{\partial x\partial y}\right)=\upsilon_{nf}\frac{\partial^2 u}{\partial y^2}-\frac{\sigma_{nf}B_o^2}{\rho_{nf}}\left(u+\lambda_1 v\frac{\partial u}{\partial y}\right)$$

$$-\frac{\upsilon_{nf}}{K}u-Fu^2 \tag{2}$$

$$u\frac{\partial T}{\partial x}+v\frac{\partial T}{\partial y}=\alpha_{nf}\left(\frac{\partial^2 T}{\partial y^2}\right)+\frac{(\rho c)_p}{(\rho c)_{nf}}\left((D_B)_{nf}\frac{\partial T}{\partial y}\frac{\partial C}{\partial y}+\frac{(D_T)_{nf}}{T_m}\left(\frac{\partial T}{\partial y}\right)^2\right) \quad (3)$$

$$u\frac{\partial C}{\partial x}+v\frac{\partial C}{\partial y}=(D_B)_{nf}\left(\frac{\partial^2 C}{\partial y^2}\right)+\frac{(D_T)_{nf}}{T_m}\left(\frac{\partial^2 T}{\partial y^2}\right) \quad (4)$$

With the boundary conditions [18],

$$u=u_w(x)=ax, v=0, -k\frac{\partial T}{\partial y}=h_f\left(T_f-T\right), (D_B)_{nf}\frac{\partial C}{\partial y}+\frac{(D_T)_{nf}}{T_m}\frac{\partial T}{\partial y}=0 \; at \quad y=0\,,$$

$$u\to 0, T\to T_\infty\,, C\to C_\infty \; as \; y\to\infty \quad (5)$$

where, v and u denote the respective flow velocities in the vertical and horizontal directions, ρ_{nf} characterises the nanofluid density, λ_1 signifies the relaxation time, $\upsilon_{nf}=\left(\mu_{nf}/\rho_{nf}\right)$ represents the kinematic viscosity, μ_{nf} symbolises the dynamin viscosity, σ_{nf} signifies the electrical conductivity, K defines the permeability of porous medium, $F=C_b/x\sqrt{K}$ represents the non-uniform inertia coefficient of porous medium, C_b denotes the drag coefficient, $(\rho c)_p$ defines nanoparticles' effective heat capacity, $\alpha_{nf}=((k_{nf})/\left(\rho c_p\right)_{nf})$ corresponds to the thermal diffusivity, k_{nf} stands for the thermal conductivity, $\left(\rho c_p\right)_{nf}$ denotes heat capacity of nanofluid, $(D_B)_{nf}$ symbolises Brownian diffusivity, C represents concentration, T_∞ corresponds to the ambient fluid temperature, $(D_T)_{nf}$ represents thermophoretic diffusion coefficient and C_∞ characterises the ambient fluid concentration and a positive constant [19-21].

$$\rho_{nf}=(1-\xi)\rho_f+\xi\rho_s \;;\mu_{nf}=\frac{\mu_f}{(1-\xi)^{2.5}};(\rho C_p)_{nf}=(1-\xi)\left(\rho C_p\right)_f+\xi\left(\rho C_p\right)_s;[22]$$

$$\alpha_{nf}=\frac{k_{nf}}{\left(\rho C_p\right)_{nf}},\frac{k_{nf}}{k_f}=\left\{\frac{(k_s+(l-1)k_f)-(l-1)\xi(k_f-k_s)}{(k_s+(l-1)k_f)+\xi(k_f-k_s)}\right\};\sigma_{nf}=\left(1+\frac{3.\left(\frac{\sigma_s}{\sigma_f}-1\right)\xi}{\left(\frac{\sigma_s}{\sigma_f}+2\right)-\left(\frac{\sigma_s}{\sigma_f}-1\right)\xi}\right);$$

$$(D_B)_{nf}=(1-\xi)(D_B)_f;(D_T)_{nf}=(1-\xi)(D_T)_f \quad (6)$$

And considering,

$$u=axf'(\eta), v=-\sqrt{a\upsilon_{nf}}f(\eta), \eta=y\sqrt{a/\upsilon_{nf}}\,, \theta(\eta)=(T-T_\infty)/\left(T_f-T_\infty\right),$$
$$\phi(\eta)=(C-C_\infty)/C_\infty \quad (7)$$

By employing similarity transformation, and replacing Eq. (6) in Eq. (2)-(4), we get [23].

$$f''' + \left(\left(\frac{A_1}{1-\xi+\xi\left(\frac{\rho_S}{\rho_f}\right)}\right)M^2\beta + 1\right)ff'' + \beta(2ff'f'' - f^2f''') - \left(\left(\frac{A_1}{1-\xi+\xi\left(\frac{\rho_S}{\rho_f}\right)}\right)M^2 + \left(\frac{1}{(1-\xi)^{2.5}\left(1-\xi+\xi\left(\frac{\rho_S}{\rho_f}\right)\right)}\right)\lambda\right)f' - (1+Fr)f'^2 = 0 \quad (8)$$

$$\theta'' + \frac{k_f}{k_{nf}}\left(\frac{1-\xi+\xi\left(\frac{Cp_S}{Cp_f}\right)}{(1-\xi)^{2.5}}\right)\mathrm{Pr}f\theta' + (1-\xi)\frac{k_f}{k_{nf}}Pr(N_b\theta'\phi' + N_t\theta'^2) = 0 \quad (9)$$

$$\phi'' + \frac{k_{nf}}{k_f}\left(\frac{1}{1-\xi+\xi\left(\frac{\rho_S.Cp_S}{\rho_f.Cp_f}\right)}\right)LePrf\phi' + (N_t/N_b)\theta'' = 0 \quad (10)$$

Subject to initial and boundary conditions,

$$f(0) = 0, \qquad f'(0) = 1, \qquad \theta'(0) = -\frac{k_{nf}}{k_f}(A_2)\gamma\big(1-\theta(0)\big), \qquad N_b\phi'(0) + N_t\theta'(0) = 0$$
$$f'(\infty) \to 0, \theta(\infty) \to 0, \phi(\infty) \to 0 \quad (11)$$

Here, M represents magnetic parameter, λ defines porosity parameter, β implies Deborah number, N_b denotes Brownian motion parameter, N_t signifies thermophoresis parameter, (Pr) represents Prandtl number, Fr defines inertia coefficient (Forchheimer number), γ denotes the Boit number and Le signifies Lewis number. These variables are expressed as stated below.

$$M^2 = \frac{\sigma_f B_o^2}{\rho_f}, \beta = a\lambda_1, \lambda = \frac{\upsilon_f}{Ka}, Fr = C_b/\sqrt{K}, Pr = \frac{\upsilon_f}{\alpha_f}, N_b = \frac{(\rho c)_p (D_B)_f (C_\infty)}{(\rho c)_f \nu_f}$$
$$N_t = \frac{(\rho c)_p D_T (T_f - T_\infty)}{(\rho c)_f \nu_f T_\infty}, \gamma = \frac{h_f}{K}\sqrt{\frac{\upsilon_f}{a}}, Le = \frac{\alpha_f}{D_B}, A_1 = \left(1 + \frac{3.\left(\frac{\sigma_S}{\sigma_f}-1\right)\xi}{\left(\frac{\sigma_S}{\sigma_f}+2\right)-\left(\frac{\sigma_S}{\sigma_f}-1\right)\xi}\right),$$
$$A_2 = \frac{1}{\sqrt{(1-\xi)^{2.5}\left(1-\xi+\xi\left(\frac{\rho_S}{\rho_f}\right)\right)}} \quad (12)$$

For local Nusselt number [24],

$$Nu_x = -\frac{x}{(T_w - T_o)}\left(\frac{\partial T}{\partial y}\right)_{y=0} \Rightarrow Nu_x(Re_x)^{-1/2} = -A_2\theta'(0) \quad (13)$$

where $Re_x = u_w x/\nu$ indicates the local Reynolds number [25, 26].

3. Numerical Approach and Validation

Since a series of non-similar Eq. (8)-(10) is characterised as being nonlinear and there is no rational solution; thus, a numerical handling is considered to be more appropriate. The 4th–5th order Runge–Kutta–Fehlberg method via MAPLE [27] is employed to statistically solve such series of ordinary differential equations (ODEs), including periphery conditions (11). Eq. (8)-(10) were converted into a first order equation system by expressing as

$$\eta = y_1; f = y_2; f' = y_3; f'' = y_4; \theta = y_5; \theta' = y_6; \phi = y_7; \emptyset' = y_8 \tag{14}$$

$$\begin{bmatrix} y_1' \\ y_2' \\ y_3' \\ y_4' \\ y_5' \\ y_6' \\ y_7' \\ y_8' \end{bmatrix} = \begin{bmatrix} 1 \\ y_3 \\ y_4 \\ -\left(\frac{1}{1-\beta y_2^2}\right)\left(\begin{array}{l} 2\beta y_2 y_3 y_4 + \left(\left(\frac{A_1}{1-\xi+\xi\left(\frac{\rho_s}{\rho_f}\right)}\right)M^2\beta + 1\right)y_2 y_4 - (Fr+1)y_3^2 \\ \quad + \left(\left(\frac{A_1}{1-\xi+\xi\left(\frac{\rho_s}{\rho_f}\right)}\right)M^2 - \lambda\left(\frac{1}{(1-\xi)^{2.5}\left(1-\xi+\xi\left(\frac{\rho_s}{\rho_f}\right)\right)}\right)y_3\right) \end{array}\right) \\ y_6 \\ -\frac{k_f}{k_{nf}}\left(\frac{1-\xi+\xi\left(\frac{Cp_s}{Cp_f}\right)}{(1-\xi)^{2.5}}\right)Pry_2 y_6 - (1-\xi)\frac{k_f}{k_{nf}}Pr(N_b y_8 y_6 + N_t y_6^2) \\ y_8 \\ \frac{k_{nf}}{k_f}\left(\frac{1}{1-\xi+\xi\left(\frac{\rho_s . Cp_s}{\rho_f . Cp_f}\right)}\right)LePry_2 y_8 + \left(\frac{N_t}{N_b}\right)\frac{k_f}{k_{nf}}\left(\frac{1-\xi+\xi\left(\frac{Cp_s}{Cp_f}\right)}{(1-\xi)^{2.5}}\right)Pry_2 y_6 + \left(\frac{N_t}{N_b}\right)(1-\xi)\frac{k_f}{k_{nf}}Pr(N_b y_8 y_6 + N_t y_6^2) \end{bmatrix} \tag{15}$$

with initial conditions given below,

$$\begin{bmatrix} y_1(0) \\ y_2(0) \\ y_3(0) \\ y_4(0) \\ y_5(0) \\ y_6(0) \\ y_7(0) \\ y_8(0) \end{bmatrix} = \begin{bmatrix} 0 \\ 0 \\ 1 \\ \chi_1 \\ \chi_2 \\ -\gamma(1-\chi_1) \\ \chi_3 \\ \left(\frac{N_t}{N_b}\right)\gamma(1-\chi_1) \end{bmatrix} \tag{16}$$

Here, $[\chi_1, \chi_2, \chi_3] = [f''(\eta), \theta(\eta), \phi(\eta)]$, γ represents the Biot number. The 1st order system was statistically integrated with the 4th–5th order system by employing the Runge–Kutta–Fehlberg approach, where suitable values are assigned to χ_1, χ_2, χ_3 to perform iterative approximation pertaining to these quantities. Reiteration of the complete procedure was done for various η_{max}; for instance – $\eta = 5, 7$ until exponentially obtaining steady solutions that are inclined towards free flow conditions by making a comparison of these with MAPLE 18.

To justify the put forward numerical scheme, the current value is compared with that of [17]. As seen in Table 1, there was a high resemblance with inertia coefficient, Deborah number and Lewis number parameters, which suggests that theoretical solution of $-\theta'(0)$ is in good agreement.

Table 1
Comparative $-\theta'(0)$ for different values of Deborah number β, inertia coefficient Fr and Lewis number Le parameters with [17].

			Muhammad *et al.,*[17]	Present work
β	Fr	Le	$-\theta'(0)$	$-\theta'(0)$
0.0			0.20321	0.20322
0.5			0.19945	0.19946
1.0			0.19587	0.19591
	0.0		0.20203	0.20203
	0.5		0.20042	0.20044
	1.0		0.19895	0.19897
		0.5	0.20185	0.20183
		1.0	0.20169	0.20170
		1.5	0.20160	0.20161

Table 2
Thermos-physical properties of water and nanoparticle [28-30]

	$\rho(kg/m^3)$	$C_p(JkgK)$	$K\ (W/mk)$	$\sigma\ (\Omega^{-1}m^{-1})$	Prandtl number
Pure water	997.1	4179	0.613	5.5	6.82
Al_2O_3	3970	765	40	16.7	-

4. Graphical Discussion

We have accounted for two-dimensional steady and incompressible flow pertaining to water-based oxide aluminium to establish the nanomaterial transport mechanism. Darcy–Forchheimer relation of Maxwell nanofluid is considered for the characterisation of flow in porous space. We examined the effect of magnetic field (M =0.0 and M =2.0) on various noteworthy parameters such as Biot number, nanoparticle thermophoresis, porosity, inertia coefficient, volume fraction and Brownian motion parameters. A linear stretched surface allows creating a nanofluid flow.

Figure 1(a) and (b) is aimed at presenting the variation in Biot number with temperature as well as distribution of nanoparticle concentration with several values of magnetic field. When the heat transfer coefficient and kinematic viscosity increased cause increase of thermal boundary thickness as well as temperature. In case of nanoparticle concentration which increased with decreased of permeability and stretching surface with increase of kinematic viscosity. For increasing value pertaining to Biot number, Figure 1(a) shows that there is greater boundary layer thickness. For M=2.0, the temperature profile was found to be greater versus M=0.0. Based on Figure 1(a), increasing the temperature as well as nanoparticle concentration resulted in increased Biot number. Figure 2 shows the impact cast by Forchheimer number on the distribution of velocity. Here, the velocity was seen to decrease with rise in Forchheimer number, since the drag coefficient increased such that when magnetic field M=2.0 increased, the velocity decreased. Which magnetic cause drag for nanofluid flow.

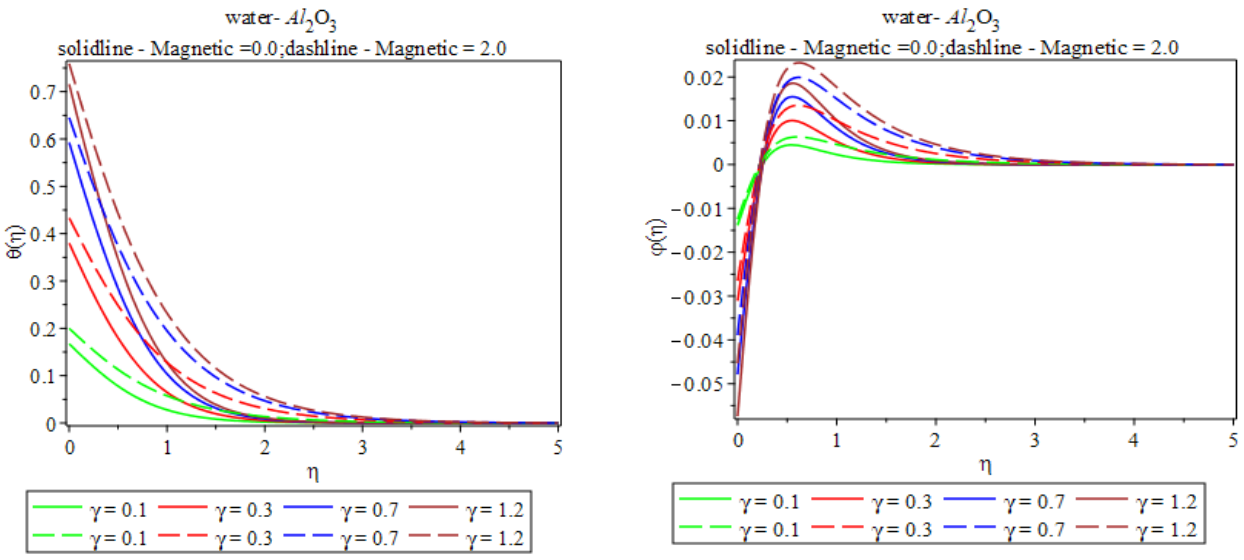

(a) (b)

Fig. 1. the effect of various Biot number on (a) temperature (b) nanoparticle concentration dimensionless when M = 0.0 and M = 2.0

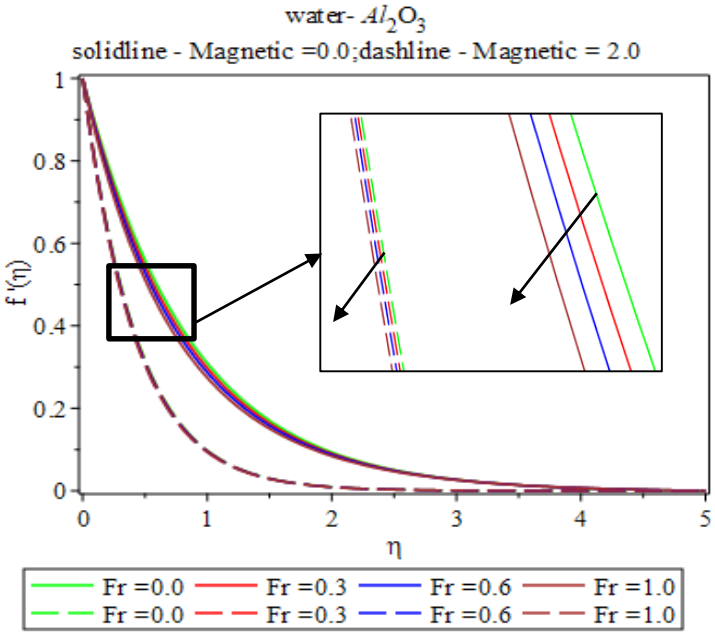

Fig. 2. The effect of various inertia parameter on (a) velocity dimensionless when M = 0.0 and M = 2.0

Figure 3 displays the effectiveness pertaining to the porosity parameter. The effect of magnetic field (M=2.0) was found to be lower for velocity, while higher for distribution of concentration and temperature. Based on Figure 3(a), the velocity was found to decrease with increase in porosity, and thickening of boundary layer follows. Increase of M=2.0 resulted in decrease in velocity distribution. As per Figure 3 (b), larger porosity parameter resulted in increased temperature profile as well as associated boundary layer with M=2.0, which is applicable to the nanoparticle concentration profile presented in Figure 4.

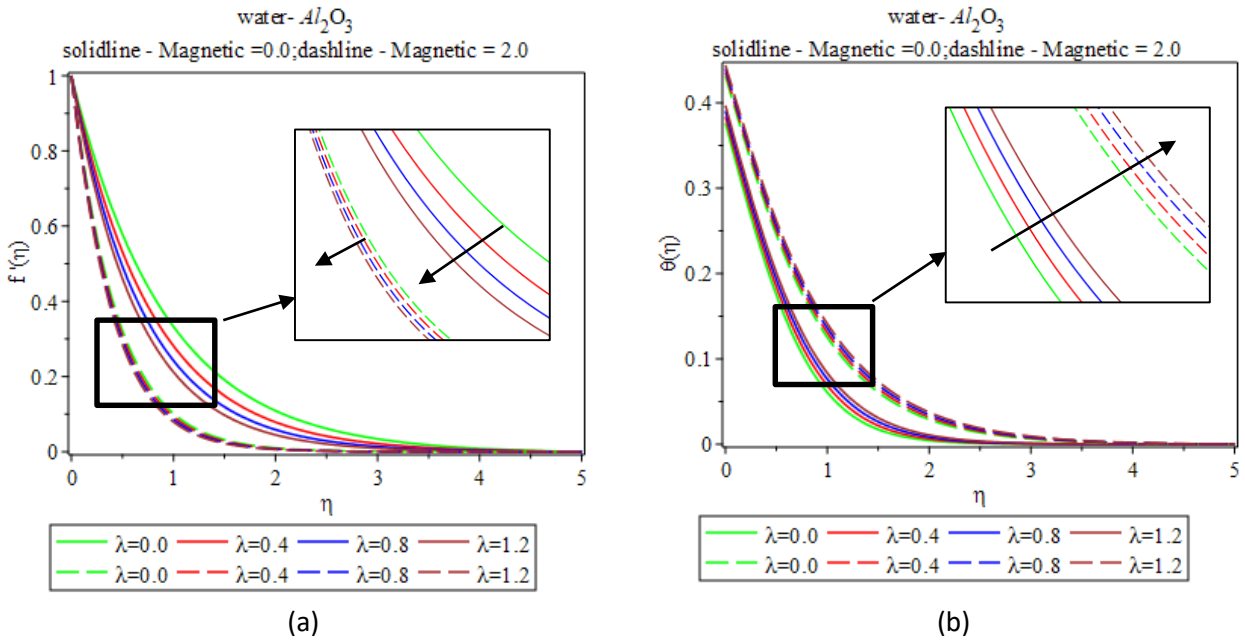

(a) (b)

Fig. 3. The effect of various porosity parameter on (a) velocity temperature dimensionless

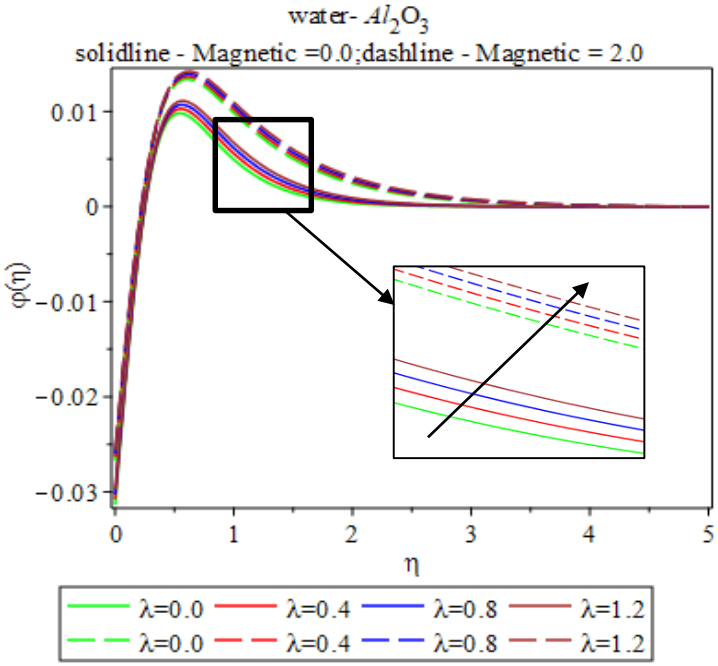

Fig. 4. The effect of various porosity parameter on nanoparticle concentration dimensionless when M = 0.0 and M = 2.0

Figure 5(a) shows that larger values pertaining to nanoparticle volume fraction result in increased temperature as well as decreased nanoparticle concentration profiles as presented in Figure 5(b). When M=2.0, there is an enhancement in nanoparticle concentration and rise in temperature. Figure 6(a) and (b) shows the effect of thermophoresis on concentration distribution and temperature. Based on Figure 6(a), rise in thermophoresis was found to cast an improved effect on the temperature profile as well as associated thermal layer thickness, and gave lower nanoparticle concentration. As per Figure 6(b), with M=2.0, it was clear that the magnetic field improved the nanoparticle concentration distribution as well as temperature.

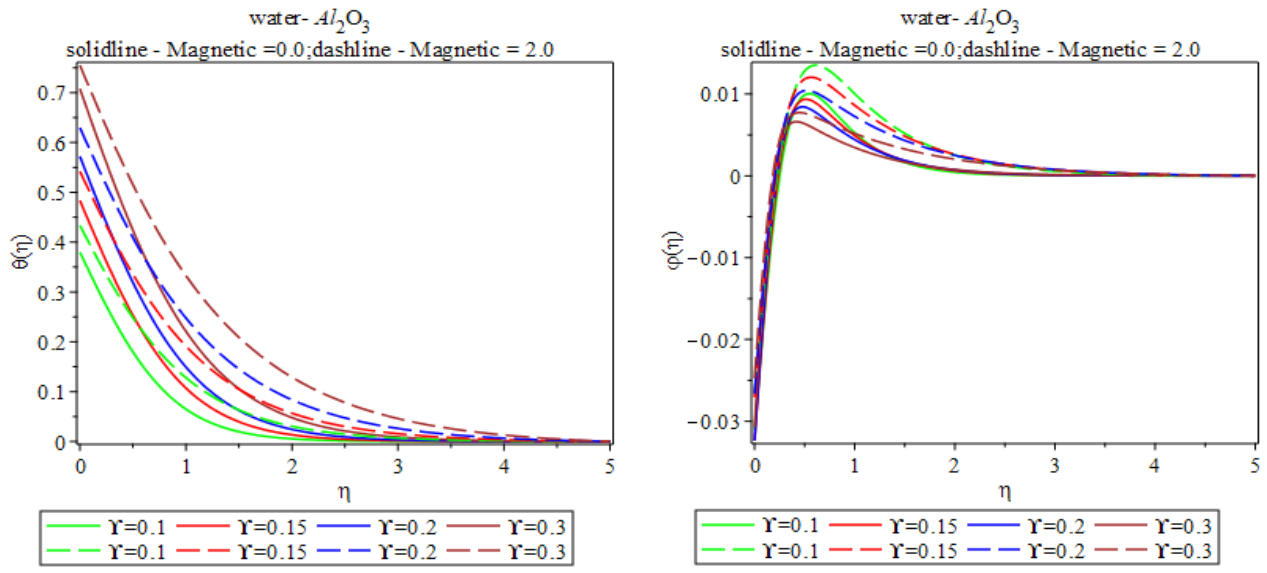

(a) (b)

Fig. 5. The effect of various nanoparticle volume fraction on (a) temperature nanoparticle (b) concentration dimensionless when M = 0.0 and M = 2.0

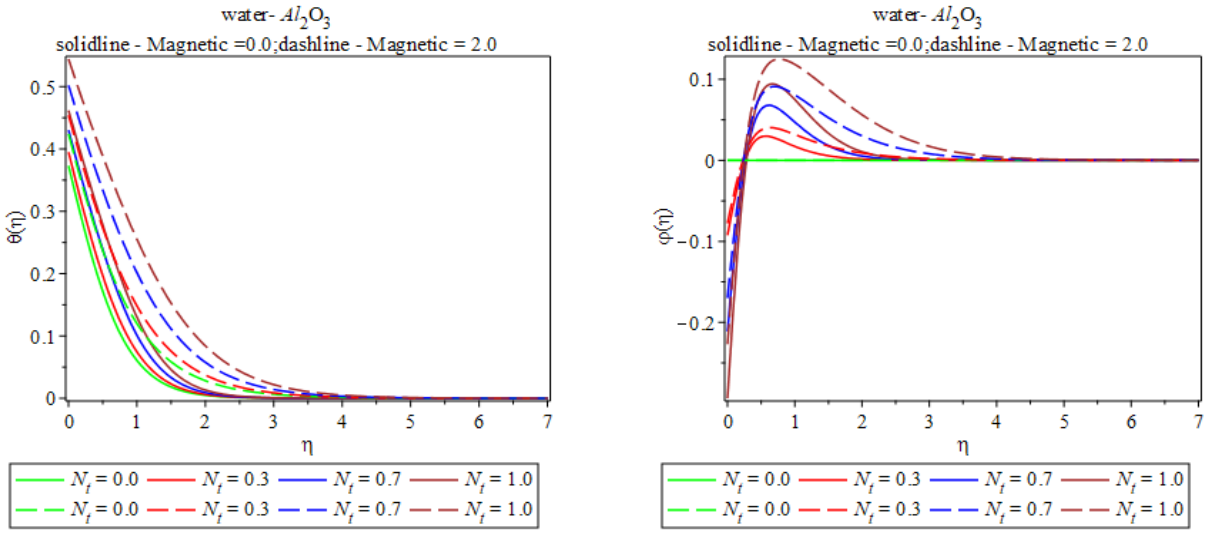

(a) (b)

Fig. 6. the effect of various thermophoresis parameter on (a) temperature nanoparticle (b) concentration dimensionless when M = 0.0 and M = 2.0

Figure 7 provides an explanation regarding the concentration field and considers the impact of Brownian motion parameter. Larger Brownian motion parameter signifies that decay has occurred in the concentration field. Under magnetic field of M=2.0, improvement in the concentration profile was observed. Figure 8 demonstrates the impact of Biot number on Nusselt number along with high and low magnetic fields. Figure 9 the effect of porosity parameters on shear stress $f''(0)$ with various magnetic field. Table 3 lists out the Nusselt number values by considering various parameters. Here, lower heat transfer rate is associated with larger values for thermophoresis parameters, while the value remains constant when it comes to Brownian motion.

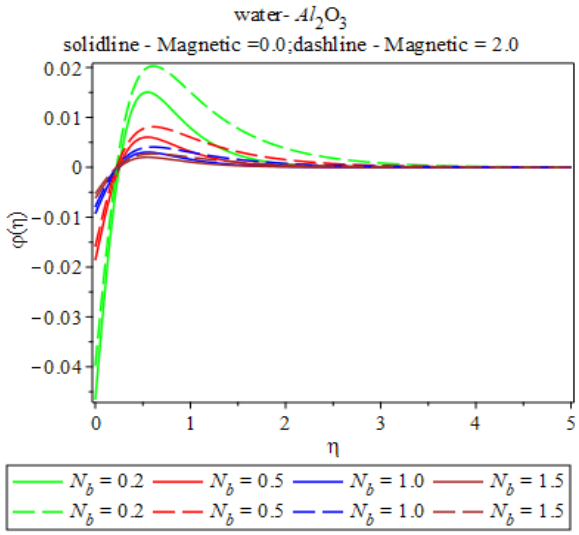

Fig. 7. The effect of various Brownian motion on nanoparticle concentration dimensionless when M = 0.0 and M = 2.0

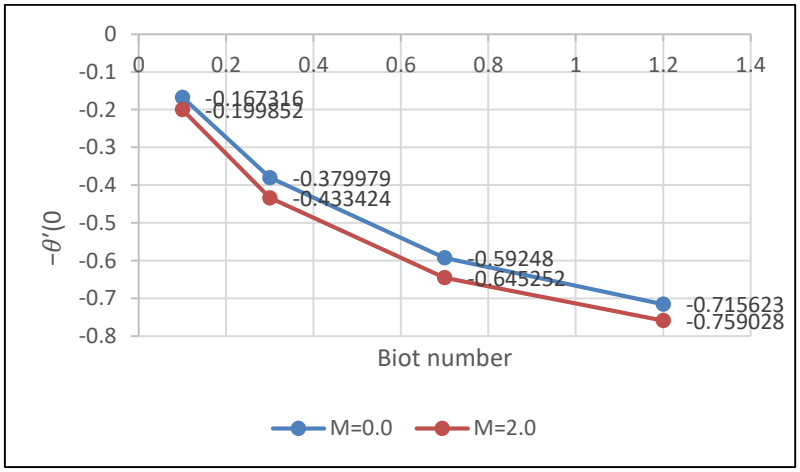

(a)

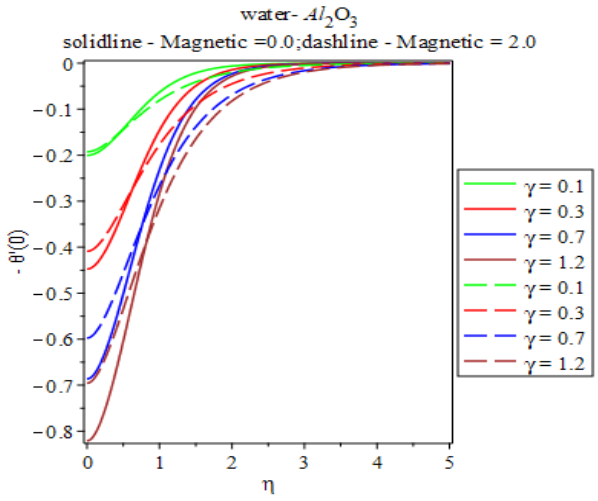

(b)

Fig. 8. The effect of different Biot number parameter on Nusselt number $(Nu_x(Re_x)^{-1/2})/A_2 = -\theta'(0)$ (i e. the rate of heat transfer) with various magnetic field (M = 0.0 and M = 2.0)

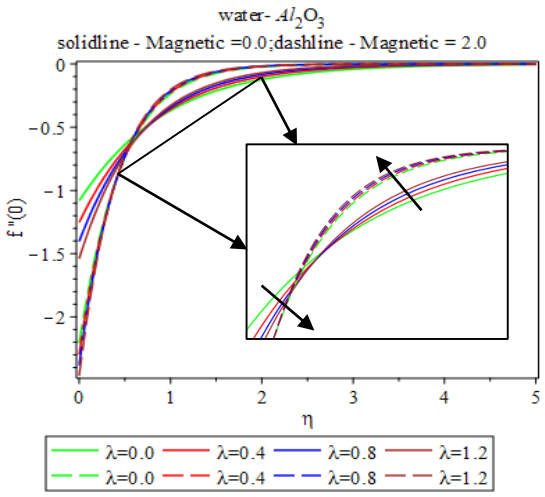

Fig. 9. The effect of porosity parameters on shear stress $f''(0)$ with various magnetic field

Table 3
Nusselt number with the effect of $\lambda, Fr, \Upsilon, N_b, N_t \quad \beta = 0.2, Le = 1.0, \Pr = 6.82$ and using lamina (16.1576) as a nanoparticle shape

					$Nu_x(Re_x^{-1/2})$	
λ	Fr	Υ	N_b	N_t	M = 0.0	M = 2.0
0.0	0.1	0.1	0.3	0.1	-0.376161	-0.431225
0.4					-0.383612	-0.435583
0.8					-0.390413	-0.439782
1.2					-0.396714	-0.443835
0.2	0.0	0.1	0.3	0.1	-0.379147	-0.432999
	0.3				-0.381598	-0.434265
	0.6				-0.383921	-0.435506
	1.0				-0.386848	-0.437122
0.2	0.1	0.1	0.3	0.1	-0.379979	-0.433424
		0.15			-0.483655	-0.542044
		0.2			-0.572103	-0.629562
		0.3			-0.707707	-0.755011
0.2	0.1	0.1	0.2	0.1	-0.379979	-0.433424
			0.5		-0.379979	-0.433424
			1.0		-0.379979	-0.433424
			1.5		-0.379979	-0.433424
0.2	0.1	0.1	0.3	0.0	-0.373031	-0.424213
				0.3	-0.394907	-0.454074
				0.7	-0.430086	-0.502070
				1.0	-0.461832	-0.544233

5. Conclusion

The steady two-dimensional (2D) stretched flow pertaining to Tiwari-Das nanofluid has been evaluated. The porous space is saturated via an incompressible nanofluid, which characterises the Darcy–Forchheimer model. A convective heating process is followed to manage the surface temperature as defined by heat transfer coefficient. A uniform magnetic field was imposed and a linear stretching surface was used to generate the flow.

i. Magnetic field: If there is an increase in the magnetic field along with M=2.0, then
- The magnetic field improved the temperature distribution along with the impact of Biot number, nanoparticle volume fraction, porosity and thermophoresis parameters.
- Velocity distribution is decreased with porosity and Forchheimer number parameters.
- The concentration field is improved along with the impact of Biot number, nanoparticle volume fraction, porosity, Brownian motion and thermophoresis parameters.

i. Velocity profile where (M=0.0): The velocity distribution is decreased when there is an increase in the Forchheimer number and porosity parameters.
ii. Temperature profile where (M=0.0): When there is an increase in Biot number, improvement in thermophoresis, temperature distribution and nanoparticle volume fraction parameters occur.
iii. Concentration field where (M=0.0): When there is an increase in Biot number, there is enhancement in concentration field. Moreover, there is a decrease with rise in Brownian motion and nanoparticle volume fraction.

References

[1] Choi, Stephen US, and Jeffrey A. Eastman. *Enhancing thermal conductivity of fluids with nanoparticles*. No. ANL/MSD/CP-84938; CONF-951135-29. Argonne National Lab., IL (United States), 1995.
[2] Khan, Arshad, Dolat Khan, Ilyas Khan, Farhad Ali, Faizan ul Karim, and Muhammad Imran. "MHD flow of Sodium Alginate-based Casson type nanofluid passing through a porous medium with Newtonian heating." *Scientific reports* 8, no. 1 (2018): 8645.
[3] Shehzad, S. A., F. M. Abbasi, T. Hayat, and A. Alsaedi. "Cattaneo-Christov heat flux model for Darcy-Forchheimer flow of an Oldroyd-B fluid with variable conductivity and non-linear convection." *Journal of Molecular Liquids* 224 (2016): 274-278.
[4] Hayat, T., M. Zubair, M. Waqas, A. Alsaedi, and M. Ayub. "Importance of chemical reactions in flow of Walter-B liquid subject to non-Fourier flux modeling." *Journal of Molecular Liquids* 238 (2017): 229-235.
[5] Sadiq, M. A., M. Waqas, and T. Hayat. "Importance of Darcy-Forchheimer relation in chemically reactive radiating flow towards convectively heated surface." *Journal of Molecular Liquids* 248 (2017): 1071-1077.
[6] P. Forchheimer, "Wasserbewegung durch boden," *Z. Ver. Deutsch, Ing.,* vol. 45, pp. 1782-1788, 1901.
[7] Muskat, Morris. "The flow of homogeneous fluids through porous media." *Soil Science* 46, no. 2 (1938): 169.
[8] Hayat, T., Taseer Muhammad, Saleh Al-Mezal, and S. J. Liao. "Darcy-Forchheimer flow with variable thermal conductivity and Cattaneo-Christov heat flux." *International Journal of Numerical Methods for Heat & Fluid Flow* 26, no. 8 (2016): 2355-2369.
[9] Hayat, Tasawar, Farwa Haider, Taseer Muhammad, and Ahmed Alsaedi. "On Darcy-Forchheimer flow of viscoelastic nanofluids: A comparative study." *Journal of Molecular Liquids*233 (2017): 278-287.
[10] Hayat, Tasawar, Rai Sajjad Saif, Rahmat Ellahi, Taseer Muhammad, and Bashir Ahmad. "Numerical study for Darcy-Forchheimer flow due to a curved stretching surface with Cattaneo-Christov heat flux and homogeneous-heterogeneous reactions." *Results in physics* 7 (2017): 2886-2892.
[11] Hayat, Tasawar, Kiran Rafique, Taseer Muhammad, Ahmed Alsaedi, and Muhammad Ayub. "Carbon nanotubes significance in Darcy-Forchheimer flow." *Results in physics* 8 (2018): 26-33.
[12] Hayat, T., Siraj Ullah, M. Ijaz Khan, and A. Alsaedi. "On framing potential features of SWCNTs and MWCNTs in mixed convective flow." *Results in physics* 8 (2018): 357-364.
[13] Alzahrani, Abdullah K. "Importance of Darcy–Forchheimer porous medium in 3D convective flow of carbon nanotubes." *Physics Letters A* 382, no. 40 (2018): 2938-2943.
[14] Hayat, Tasawar, Farwa Haider, Taseer Muhammad, and Ahmed Alsaedi. "Darcy-Forchheimer flow with Cattaneo-Christov heat flux and homogeneous-heterogeneous reactions." *PloS one* 12, no. 4 (2017): e0174938.
[15] Hayat, Tasawar, Farwa Haider, Taseer Muhammad, and Ahmed Alsaedi. "Numerical study for Darcy-Forchheimer flow of nanofluid due to an exponentially stretching curved surface." *Results in physics* 8 (2018): 764-771.
[16] Meraj, M. A., S. A. Shehzad, T. Hayat, F. M. Abbasi, and A. Alsaedi. "Darcy-Forchheimer flow of variable conductivity Jeffrey liquid with Cattaneo-Christov heat flux theory." *Applied Mathematics and Mechanics* 38, no. 4 (2017): 557-566.

[17] Muhammad, Taseer, Ahmed Alsaedi, Sabir Ali Shehzad, and Tasawar Hayat. "A revised model for Darcy-Forchheimer flow of Maxwell nanofluid subject to convective boundary condition." *Chinese Journal of Physics* 55, no. 3 (2017): 963-976.
[18] Chan, Sze Qi, Fazlina Aman, and Syahira Mansur. "Bionanofluid Flow Through a Moving Surface Adapting Convective Boundary Condition: Sensitivity Analysis."
[19] Ali, Farhad, Ilyas Khan, Nadeem Ahmad Sheikh, Madeha Gohar, and I. Tlili. "Effects of Different Shaped Nanoparticles on the Performance of Engine-Oil and Kerosene-Oil: A generalized Brinkman-Type Fluid model with Non-Singular Kernel." *Scientific reports* 8, no. 1 (2018): 15285.
[20] Jawad, Muhammad, Zahir Shah, Saeed Islam, Ebenezer Bonyah, and Aurang Zeb Khan. "Darcy-Forchheimer flow of MHD nanofluid thin film flow with Joule dissipation and Navier's partial slip." *Journal of Physics Communications* 2, no. 11 (2018): 115014.
[21] Kumaresan, E., A. G. Vijaya Kumar, and B. Rushi Kumar. "An exact solution on unsteady MHD free convection chemically reacting silver nanofluid flow past an exponentially accelerated vertical plate through porous medium." In *Materials Science and Engineering Conference Series*, vol. 263, no. 6, p. 062018. 2017.
[22] Jamil, M., N. C. Sidik, and MNAW Muhammad Yazid. "Thermal performance of thermosyphon evacuated tube solar collector using TiO2/water nanofluid." *J. Adv. Res. Fluid Mech. Therm. Sci* 20, no. 1 (2016): 12-29.
[23] Ramzan, Muhammad, Mohsen Sheikholeslami, Maria Saeed, and Jae Dong Chung. "On the convective heat and zero nanoparticle mass flux conditions in the flow of 3D MHD Couple Stress nanofluid over an exponentially stretched surface." *Scientific reports* 9, no. 1 (2019): 562.
[24] Noh, N. M., A. Fazeli, and NA Che Sidik. "Numerical simulation of nanofluids for cooling efficiency in microchannel heat sink." *J. Adv. Res. Fluid Mech. Therm. Sci.* 4, no. 1 (2014): 13-23.
[25] Hayat, Tasawar, Arsalan Aziz, Taseer Muhammad, and Ahmed Alsaedi. "Darcy–Forchheimer three-dimensional flow of Williamson nanofluid over a convectively heated nonlinear stretching surface." *Communications in Theoretical Physics*68, no. 3 (2017): 387.
[26] Zaimi, Khairy, Anuar Ishak, and Ioan Pop. "Boundary layer flow and heat transfer over a nonlinearly permeable stretching/shrinking sheet in a nanofluid." *Scientific Reports* 4 (2014): 4404.
[27] Ghadikolaei, S. S., Kh Hosseinzadeh, and D. D. Ganji. "Investigation on three dimensional squeezing flow of mixture base fluid (ethylene glycol-water) suspended by hybrid nanoparticle (Fe3O4-Ag) dependent on shape factor." *Journal of Molecular Liquids* 262 (2018): 376-388.
[28] Sidik, NA Che, and A. Safdari. "Modelling of convective heat transfer of nanofluid in inversed L-shaped cavities." *J. Adv. Res. Fluid Mech. Therm. Sci.* 21, no. 1 (2016): 1-16.
[29] Esfahani, Javad Abolfazli, and Vahid Bordbar. "Double diffusive natural convection heat transfer enhancement in a square enclosure using nanofluids." *Journal of Nanotechnology in Engineering and Medicine* 2, no. 2 (2011): 021002.
[30] Roşca, Natalia C., and Ioan Pop. "Axisymmetric rotational stagnation point flow impinging radially a permeable stretching/shrinking surface in a nanofluid using Tiwari and Das model." *Scientific reports* 7 (2017): 40299.